

# Design and measurement methods for a lithium vapor box similarity experiment<sup>a)</sup>

J. A. Schwartz,<sup>1, b)</sup> E. D. Emdee,<sup>1</sup> M. A. Jaworski,<sup>2</sup> and R. J. Goldston<sup>1</sup>

<sup>1)</sup>Princeton University, Princeton, New Jersey 08540, USA

<sup>2)</sup>Princeton Plasma Physics Laboratory, Princeton, New Jersey 08543-0451, USA

(Dated: August 10, 2018)

The lithium vapor box divertor is a concept for handling the extreme divertor heat fluxes in magnetic fusion devices. In a baffled slot divertor, plasma interacts with a dense cloud of Li vapor which radiates and cools the plasma, leading to recombination and detachment. Before testing on a tokamak the concept should be validated: we plan to study detachment and heat redistribution by a Li vapor cloud in laboratory experiments. Mass changes and temperatures are measured to validate a Direct Simulation Monte Carlo model of neutral Li. The initial experiment involves a 5 cm diameter steel box containing 10 g of Li held at 650°C as vapor flows out a wide nozzle into a similarly-sized box at a lower temperature. Diagnosis is made challenging by the required material compatibility with lithium vapor. Vapor pressure a steep function of temperature, so to validate mass flow models to within 10%, absolute temperature to within 4.5 K is required. The apparatus is designed to be used with an analytical balance to determine mass transport. Details of the apparatus and methods of temperature and mass flow measurements are presented.

Keywords: lithium, divertor, detachment, vapor

## I. INTRODUCTION

The divertor heat flux in future toroidal fusion reactors will likely require a detached plasma<sup>1</sup>. While experiments on present tokamaks have demonstrated detachment via gas puffs,<sup>2</sup> gas may build up in the divertor and cause the detachment front to move upstream, ending in a MARFE and/or disruption<sup>3,4</sup>. A method of producing stable detachment is required, such as the lithium vapor box (LVB) divertor<sup>5,6</sup>.

Before testing on a toroidal device, properties and behavior of the LVB can be tested on a smaller scale, such as a linear divertor test facility<sup>7</sup>. Key parameters are the density of Li vapor necessary for detachment, the dispersal of the plasma heat flux during detachment, the amount of Li carried upstream through the plasma, and the amount of neutral Li efflux to the main chamber, some of which can be studied in linear plasma devices.

A preliminary experiment at PPPL has been designed to measure Li efflux without plasma present, as would be between plasma discharges. This is done in order to validate a Direct Simulation Monte Carlo<sup>8,9</sup> (DSMC) code SPARTA<sup>10</sup> for use with evaporating and condensing lithium systems in the transitional flow regime.

The experimental device, scaled with flow parameters relevant to those that would be found on a tokamak, is a linear string of three 5 cm-diameter cylindrical boxes, each heated to different temperatures up to > 900 K. An initial quantity of Li, 10 g, is placed in the hottest of the boxes, where it evaporates and condenses in the cooler boxes. Lithium is reactive and corrosive to many

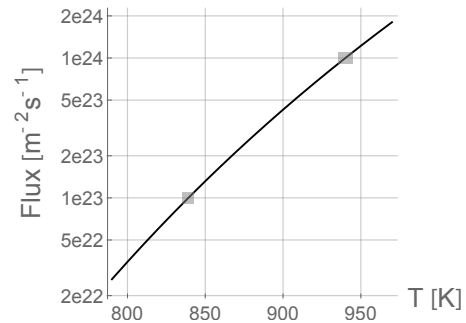


Figure 1. Equilibrium Li vapor flux  $\Gamma$  (Equation 1) at temperatures relevant to the hottest box. Gray rectangles show the temperature range for a  $\pm 10\%$  range in  $\Gamma$ .

materials, so it is difficult to directly monitor properties of the vapor flow inside the device. Instead, the boxes are weighed before and after a high temperature cycle to determine the mass transferred. Flow rates are deduced from the mass change  $\Delta m$  over a duration  $\Delta t$ . The boxes are designed to separate to be weighed. Estimates of flow rates in Reference 5 show reductions by an order of magnitude per box and typical flow rates of a few  $\text{mg s}^{-1}$ , so lightweight boxes and accurate mass change measurements are necessary. Mass flow rates in the device are a strong function of temperature: as shown in Figure 1, a 4 K surface temperature change at 873 K produces an increase in vapor flux of 10%. A 21-channel thermocouple (TC) system is used to measure box wall temperatures.

Details of the experimental design including lightweight, separable boxes and considerations for the design of the TC system and error estimates are discussed below.

<sup>a)</sup>Contributed paper published as part of the Proceedings of the 22nd Topical Conference on High-Temperature Plasma Diagnostics, San Diego, California, April, 2018.

<sup>b)</sup>Electronic mail: jschwart@pppl.gov

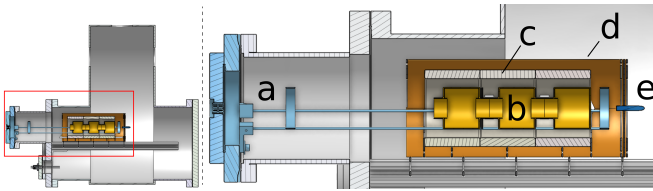


Figure 2. Left, a cross section of the apparatus. Right, detail of red rectangle. (a) In blue, a flange attached to a 50-pin electrical feedthrough and to rods that support the boxes. (b) In yellow, three vapor boxes. The ‘box 1’, at right, is hottest. Vapor will flow from right to left. Parts (a) and (b) are moved to and from the glovebox together. (c) In white, the three ceramic radiant heaters. (d) In orange, the SS shim stock ‘outer shield’. (e) In dark blue, the gas feed tube (right end curved out of the plane).

## II. THEORY AND REQUIREMENTS

A simple model for divertor power dissipation<sup>6</sup> assumes that a divertor leg surrounded by vapor experiences an inward flux of neutral atoms and a constant amount of cooling per atom,  $\epsilon_c$ .

Depending on power, geometry and  $\epsilon_c$  (see Equation 2 of Reference 6), Li vapor number fluxes to extinguish a DEMO divertor plasma are estimated to be of magnitude  $5 \times 10^{22} \text{ m}^{-2}\text{s}^{-1}$  to  $6 \times 10^{24} \text{ m}^{-2}\text{s}^{-1}$ , corresponding to one-way fluxes (defined below) of equilibrium vapor with temperatures of 800 K to 1100 K respectively.

The one-way flux  $\Gamma$  through a surface of an equilibrium ideal gas is given by

$$\Gamma = \frac{1}{4} n \bar{v} = \frac{p}{\sqrt{2\pi m k_b T}} \quad (1)$$

with  $\Gamma$  in  $\text{m}^{-2}\text{s}^{-1}$ , density  $n$  in  $\text{m}^{-3}$ , average velocity  $\bar{v}$  in  $\text{m/s}$ , pressure  $p$  in Pa, molecular mass  $m$  in kg,  $T$  in K, and Boltzmann constant  $k_b$ .

Li vapor pressure  $p_{\text{Li}}(T)$  is a steep function of temperature<sup>11–14</sup> and at temperatures relevant to this experiment,  $\delta\Gamma/\Gamma > \delta T/T$ . For example, errors  $\delta T$  for which  $\delta\Gamma = 10\%$ ,  $\Gamma(T_0 + \delta T)/\Gamma(T_0) = 1.1$ , range from 3.5 K at 815 K and 4.5 K at 920 K to 5.8 K at 1037 K.

The vapor box operates in regimes of intermediate Knudsen number,  $\text{Kn} = \lambda_{\text{MFP}}/L$  from 0.01 to 1. In this transitional flow regime, DSMC models are more accurate than fluid models since they simulate particles with finite mean free paths. A DSMC model for the vapor box using the code SPARTA<sup>10</sup> is under development. The typical scale of vapor pressures, flows through the device and evaporation fluxes are set by  $p_{\text{Li}}(T)$  and  $\Gamma$ .

Therefore, validation of flow rates computed with DSMC to 10% using an experiment with a first box at 920 K will require measurements of mass flow through the boxes to better than 10% as well as measurements of liquid Li surface temperatures to better than  $\pm 4.5$  K.

## III. APPARATUS AND APPROACH

Figure 2 shows the design of the apparatus, in the configuration with the ‘transfer assembly’ bolted into the

Table I. Example steady state parameters for vapor box system, computed using the ‘choked flow model’<sup>5</sup> with flow reduced by 2 to match preliminary DSMC simulations.

Box number	1	2	3
Flow Knudsen number	0.0448	0.136	0.435
Box temperature [K]	919	849	803
Heater temperature [K]	1071	774	778
Box emissivity	0.3	0.85	0.85
Heater emissivity	0.85	0.85	0.85
Initial Li load [g]	10	0	0
Lithium efflux [mg/s]	4.0	1.2	0.36
Over 30 minutes [g]	7.1	2.2	0.66
Net $\Delta m$ [g]	-7.1	+5.0	+1.5
Net latent heat flow [W]	-91	+63	+19

vacuum chamber. The transfer assembly, (a) and (b) in the image, is composed of the Li-containing boxes, a 50-pin electrical feedthrough, and supports to hold up the boxes. This high-pin-count feedthrough has pins made of a Be-Cu alloy. During an experiment the transfer assembly is moved from an argon glovebox to the vacuum chamber and back. First in the glovebox, 10 g of solid Li is placed in ‘box 1’ shown on the right of the image. Each box is weighed to establish an initial mass. The boxes are joined together and placed on the transfer assembly. Then in the vacuum chamber, the boxes are heated by radiant heaters (c), held for a ‘temperature soak’ period of typically 30 minutes while Li flows from box 1 to the other boxes and out, then cooled by a He gas feed from the tube (e). Finally the transfer assembly is moved back to the glovebox, and the boxes are separated and reweighed to determine  $\Delta m$ .

As shown in Equation 2, the total mass change is equal to the integral of the difference of flows in and out of the box over the heating-cooling cycle.

$$\Delta m = \int (\dot{m}_{\text{in}} - \dot{m}_{\text{out}}) dt \quad (2)$$

Typical experimental parameters are given in Table I. The justification for the design follows.

Liquid Li is a highly reactive substance, but is compatible with stainless steel 304 (SS), a common alloy. The  $\Delta m$  over time method allows all Li-facing surfaces to be made of SS, with no need for windows into the vapor-filled container. The method also imposes three constraints: the weighed boxes should be as light as possible relative to  $\Delta m$ , the boxes must be separable in order to be weighed individually, and the boxes must be heated and cooled quickly to minimize flow during the transient periods. In addition, the initial Li load (and therefore required soak time) should be minimized for safety.

Figure 3 shows a detail of the box. The box walls are 1 to 1.5 mm thick SS. There is one ‘end box’ and two ‘central boxes’. The outer diameter of the main cylinder and nozzles are 57.2 mm, and 28.6 mm, respectively. The total length of a central box is 76.2 mm.

Between boxes are butt joints, wrapped in 0.05 mm SS shimstock to prevent vapor leakage. Joint regions have a high-emissivity coating (Aremco 840-M) painted on to keep them hotter than the previous box and prevent

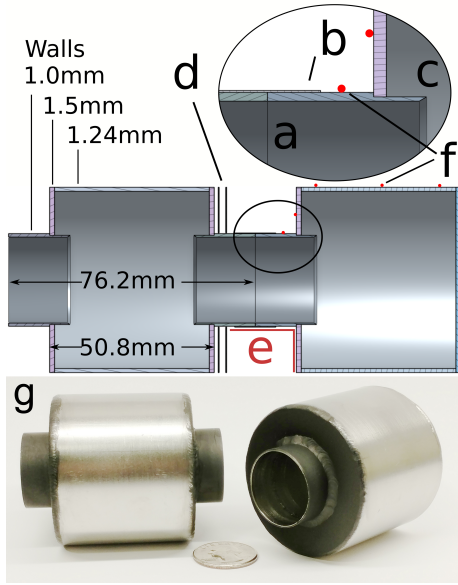


Figure 3. Design features of the vapor boxes. (a) Butt joint between boxes, to allow separation. Other joints are welded. (b) 0.05 mm SS shimstock wrapped around joint for friction. (c) Nozzle inner protrusion with knife edge, to prevent liquid Li wicking through the joint. (d) SS shim stock reflective shields. (e) Lines: high-emissivity coatings keep the joint region hot to prevent condensation. (f) Dots: example TC tip locations. (g) Photo with US quarter for scale.

condensation. To prevent *liquid* Li wicking through the joint, a knife edge protrudes inward from the nozzle.

Each box is instrumented by up to 7 permanently-attached TCs, chosen for their small size, low wire count, and accuracy at high temperatures. There are Macor connectors in the TC circuit between the boxes and feedthrough so the boxes can be weighed separately.

Including the TCs and connectors, the end and central boxes weigh 160 and 165 g, respectively.

The boxes are heated by thermal radiation to save weight: no bond to a heater is required. The heaters (Thermcraft, Inc, model RH251, similar to those on LITER<sup>15</sup>) have rated power 720 W per cylindrical segment. The inner faces are coated (Aremco 840-C) for high emissivity. The box and heater lengths are equal so that temperatures of each box can be independently controlled. In the space between the boxes and heaters, TC wires are routed and gas flows during cooling.

Outside the heaters is a cylindrical SS shim stock ‘outer shield’, Figure 2 (d), of diameter 143 mm and thickness 0.25 mm. It is a physical support for the heaters, thermal radiation shield, and duct for the cooling gas.

A gas feed of He or Ar is supplied by a tube near the hottest box, Figure 2 (e). The system is designed for a He flow rate of 80 standard L/min to cool down the boxes after the temperature soak phase. An Ar purge prevents oxidation of Li surfaces during transfer assembly insertion and removal. The chamber is pumped by a 780 L/min roughing pump during He flow and by a 500 L/s turbopump during the heating and soak phases.

#### IV. MEASUREMENT SYSTEMS AND ERRORS

Thermocouples (TCs) are used to measure temperatures of the boxes. The system has 32 channels, up to 25 of which are measurements on the transfer assembly. Type N TCs are used throughout the system for their stability compared to Type K<sup>16,17</sup>. ‘Special limits of error’ (SLE) grade material<sup>18</sup> is used when available. Inside the vacuum feedthrough, the wires are made into three bundles of 7 TCs each: one for each box. Pairs of Macor 15-pin subminiature-D connectors allow the boxes to be weighed separately. Finer wires at the readers and hot junction reduce thermal shunting, while thicker wires minimize circuit resistance. The grounded probes are sheathed in ‘Omegaclad XL’ for greater drift stability compared to SS or Inconel sheathed TCs. The tips are spot welded to the boxes beneath a small cover of SS shimstock to decrease influence on measured temperature by thermal radiation.

An analytical balance, Mettler Toledo MS-603-TS, is used to weigh the boxes. It has specified maximum weight of 620 g, readability and repeatability of 1 mg and minimum sample weight of 140 mg.

##### A. Thermocouple Measurement Errors

Each component of the system can cause errors. The National Instruments 9214 reader has errors due to cold junction compensation (CJC) as well as noise, amplifier gain and offset. Preliminary tests using a TC calibrator (Omega CL543B) show no deviations larger than 0.2 K. Variation may occur between experiments, and can be tested by repeated calibrations.

In each circuit are several lengths of TC wire. The SLE specification for Type N at 923 K is  $\pm 0.4\%$  of reading:  $\pm 2.6$  K. This can be improved by calibration: we plan to purchase TC probes with NIST-traceable calibration to  $\pm 0.8$  K at 923 K. Each lead wire segment also requires calibration. Four segments, each with two ends, plus the cold end of the probe, each calibrated to  $\pm 0.2$  K sum in quadrature to  $\pm 0.6$  K. Temperature differences across the Be-Cu alloy feedthrough pins can be subtracted by a circuit through a TC-material feedthrough<sup>19</sup>. The error in subtraction is estimated equal to the NI 9214 read error. The feedthrough temperature difference can be cross-checked by measurements of temperature on inner and outer feedthrough surfaces made by another method, such as resistance temperature detectors.

Drifts in base-metal TCs occur over hours to weeks, depending on construction, temperatures and environmental conditions, and generally cannot be determined by a recalibration<sup>18</sup>. Estimates for drifts due to reversible changes<sup>20</sup>, thermal cycling<sup>21</sup>, and irreversible changes<sup>22</sup> are shown in Table II.

Li evaporation will cool box wall inner surfaces relative to outer ones. With the expected (Table I) 90 W power flow, assumed through only the main cylindrical surface, and SS thermal conductivity<sup>23</sup> of  $25 \text{ W m}^{-1} \text{ K}^{-1}$ , the temperature difference is 0.5 K, with estimated error 0.2 K.

Table II. Estimated uncertainties in the thermocouple system. Uncertainties are treated as systematic with the exception of the first, marked <sup>R</sup> for random.

Source	Uncertainty [K]
NI 9214 reader	0.2 <sup>R</sup>
Cancellation of $\Delta T$ across feedthrough pins	0.2
Probe (NIST-traceable calibration at 923 K)	0.8
Wires (quadrature of 9 calibrations to $\pm 0.2$ K)	0.6
Reversible changes at 923 K, 100 hours <sup>20</sup>	1
After 30 cycles to 1360 K <sup>21</sup>	0.9
Irreversible changes at 923 K, 100 hours <sup>22</sup>	0.2
Box wall $\Delta T$ between outer and inner surfaces	0.2
Estimated thermal shunting	0.5
Sum	4.6

TC cable between a box and heater absorbs radiation, causing thermal shunting to the hot junction. Absorbed heat and thermal gradients can be reduced by reflective shielding and by spot welding multiple locations along the TC to the box. A test stand is being used to refine error estimates, listed as 0.5 K.

Contributions to total uncertainty are summarized in Table II. The sum, 4.6 K, is larger than the 4.5 K required to model flow to 10%, so better quantification of systematic errors and correlations, through modeling and experience with the test system, will be required.

## B. Mass measurement errors

During transfer between the vacuum chamber and glovebox the boxes will be filled with Ar. The last box will be plugged with a stopper, but air leaks through joints may oxidize Li surfaces.

A study on sorption of atmospheric gases by bulk Li metal<sup>24</sup> measured mass gain rates in room temperature, artificial dry air of roughly  $0.2 \text{ mg cm}^{-2} \text{ h}^{-1}$ .

The boxes have an internal surface area of  $150 \text{ cm}^2$ . If 6 min elapses during transfer from the vacuum chamber to the glovebox and the gas is as dry as the artificial dry air (estimated at 3.3% relative humidity<sup>24</sup>), then the mass gain per box is estimated at 3 mg. This is  $< 1\%$  of the predicted Li efflux from the third box (Table I).

Oxidation rates can be tested by repeatedly weighing boxes in air before transferring them to the glovebox.

## C. Estimation of heating and cooling times

For ease of modeling, most of the Li should flow during the temperature soak phase rather than during heating and cooling. A simple model of box 1, heater 1, and the outer shield was created. Thermal masses and emissivities (see Table I) are estimated. The heater is run at full power. Evaporative cooling from the Li flow is according to the choked flow model<sup>5</sup>. The model is integrated from initial temperatures of 300 K until box 1 reaches its operating temperature, 920 K (Table I).

In cooling, each component starts at its operating temperature. The He gas feed cools the outer box wall and

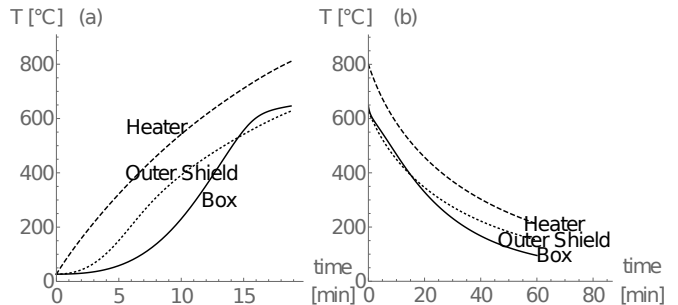


Figure 4. Simple models of box 1 (a) heating and (b) cooling. The heating model includes radiation transfer from the heaters to box and outer shield, and losses due to latent heat of evaporation from Li flowing out of box 1. The cooling model additionally includes convective cooling from a gas feed.

inner heater wall by convection<sup>25</sup>. A flow of 80 standard L/min is chosen so the He temperature rise is less than half the heater temperature. Convective cooling power is de-rated to 30% to make a conservative estimate for cooling time.

Figure 4 shows predicted temperatures during heating and cooling. Integrated Li flow during heating and cooling is 13% of that during a 30 minute temperature soak. The transient flow could be measured by an experiment with no soak time.

## V. DISCUSSION

The method of inferring mass flow by measuring mass changes of demountable boxes is motivated by the reactivity of Li with many materials.

One disadvantage is that measurements are global (integrated over wall location and time) rather than local.

Local measurements of density or flow rate by optical methods are not trivial as Li could deposit on nearby cool optics, though heated windows<sup>26</sup>, windows with helium cover gas<sup>27</sup>, or a system where the optical paths travel through high-aspect ratio tubes with heated walls and/or cold traps could be possible. Note that the experiments in Reference 26 were performed at lower temperature.

Measurements inside the boxes involving Li deposition on a small surface over time (e.g. a witness plate) can be envisioned but may require detailed knowledge of the surface temperature. Solidified Li could also prevent easy removal from a mounting surface, and protruding devices would perturb the axisymmetric geometry.

Real-time fluxes could be measured outside box 3 by measuring the electrical resistance of a thin layer of deposited liquid Li on a plate. A quartz crystal microbalance could measure vapor flux outside box 3, but vapor fluxes as well as temperatures *inside* the box are likely too high, and Li compatibility would be difficult.

Accurate measurements of box wall and liquid Li surface temperatures are required. If Type N TCs cannot meet accuracy requirements due to drifts, noble metal TCs are a fallback position. Resistance temperature detectors could be used, though they may cover



larger surface areas and the number of wires is increased. Near-infrared measurements of known-emissivity surfaces through holes drilled in the heaters are possible, but would require detailed modeling of radiation (including reflections) inside the device.

## VI. CONCLUSIONS

The design for an experiment to test Li evaporation, flow, and condensation in a vapor box geometry and to validate DSMC models has been presented.

Net flow of Li vapor into each box is measured by disassembling the string of boxes and weighing them separately in an argon glovebox. The analytical balance used is capable of weighing the 165 g boxes to a few mg, less than 1% of the expected efflux from box 3 of 700 mg.

Thermocouples outside boxes are used to infer temperatures inside box walls. Estimated errors sum to 4.6 K, larger than the  $\pm 4.5$  K corresponding to 10% changes in Li evaporation flux at 920 K. Additional work including thermal modeling and estimates of correlations between terms will be necessary to constrain errors for temperature measurements.

## ACKNOWLEDGMENTS

We acknowledge the help of expert technicians, especially A. Carpe, S. Jurczynski, G. Smalley, J. Taylor, and R. Yager, students including R. Cohen, and valuable discussions with D. Cai, T. Gray, R. Kaita, and R. Majeski. This work is supported by U.S. Department of Energy Contract No. DE-AC02-09CH11466. See <http://arks.princeton.edu/ark:/88435/dsp01bz60cz987> for the digital data in this paper.

## REFERENCES

- <sup>1</sup>R. Maingi, “Fusion energy sciences workshop on plasma materials interactions: report on science challenges and research opportunities in plasma materials interactions,” (2015).
- <sup>2</sup>A. W. Leonard, *Plasma Physics and Controlled Fusion* **60**, 044001 (2018).
- <sup>3</sup>I. H. Hutchinson, *Nuclear Fusion* **34**, 1337 (1994).
- <sup>4</sup>B. Lipschultz, F. I. Parra, and I. H. Hutchinson, *Nuclear Fusion* **56**, 056007 (2016).
- <sup>5</sup>R. J. Goldston, R. Myers, and J. A. Schwartz, *Physica Scripta* **T167**, 014017 (2016).
- <sup>6</sup>R. Goldston, A. Hakim, G. Hammett, M. Jaworski, and J. Schwartz, *Nuclear Materials and Energy* **12**, 1118 (2017).
- <sup>7</sup>H. van Eck, T. Abrams, M. van den Berg, S. Brons, G. van Eden, M. Jaworski, R. Kaita, H. van der Meiden, T. Morgan, M. van de Pol, J. Scholten, P. Smeets, G. De Temmerman, P. de Vries, and P. Zeijlmans van Emmichoven, *Fusion Engineering and Design* **89**, 2150 (2014).
- <sup>8</sup>G. A. Bird, *Annual Review of Fluid Mechanics* **10**, 11 (1978).
- <sup>9</sup>G. A. Bird, *Molecular gas dynamics and the direct simulation of gas flows* (Oxford University Press, New York, NY, 1994).
- <sup>10</sup>M. A. Gallis, J. R. Torczynski, S. J. Plimpton, D. J. Rader, T. Koehler, and J. Fan, in *AIP Conference Proceedings*, Vol. 1628 (AIP, 2014) pp. 27–36.
- <sup>11</sup>H. Davison, “Complication of thermophysical properties of liquid lithium,” NASA Technical Note NASA TN D-4650 (Lewis Research Center, Cleveland, Ohio, 1968).
- <sup>12</sup>W. T. Hicks, *The Journal of Chemical Physics* **38**, 1873 (1963).
- <sup>13</sup>M. Maucherat, *Journal de Physique et le Radium* **10**, 441 (1939).
- <sup>14</sup>P. Browning and P. E. Potter, in *Handbook of Thermodynamic and Transport Properties of Alkali Metals* (Blackwell Scientific Publications, Oxford, 1985) pp. 349–358.
- <sup>15</sup>H. Kugel, M. Bell, H. Schneider, J. Allain, R. Bell, R. Kaita, J. Kallman, S. Kaye, B. LeBlanc, D. Mansfield, R. Nygren, R. Maingi, J. Menard, D. Mueller, M. Ono, S. Paul, S. Gerhardt, R. Raman, S. Sabbagh, C. Skinner, V. Soukhanovskii, J. Timberlake, and L. Zakharov, *Fusion Engineering and Design* **85**, 865 (2010).
- <sup>16</sup>N. Burley, R. Hess, C. Howie, and J. Coleman, in *Temperature, its Measurement and Control in Science and Industry*, Vol. 5 (Washington, DC, 1982) pp. 1159–1166.
- <sup>17</sup>R. Anderson, J. Lyons, T. Kollie, W. Christie, and R. Eby, in *Temperature, its Measurement and Control in Science and Industry*, Vol. 5 (American Institute of Physics, Washington, DC, 1982) pp. 977–1007.
- <sup>18</sup>“Standard Specification for Temperature-Electromotive Force (emf) Tables for Standardized Thermocouples,” ASTM E230/E230M-17.
- <sup>19</sup>R. A. Ziemke, “Correction for Thermal EMFs in Thermocouple Feedthroughs,” NASA Tech Brief LEW-17491-1 (NASA Glenn Research Center, Cleveland, OH, 2006).
- <sup>20</sup>R. E. Bentley, *Journal of Physics D: Applied Physics* **22**, 1902 (1989).
- <sup>21</sup>A. V. Belevtsev, in *Temperature, its Measurement and Control in Science and Industry*, Vol. 7 (AIP, 2003) pp. 453–456.
- <sup>22</sup>R. E. Bentley, *Journal of Physics D: Applied Physics* **22**, 1908 (1989).
- <sup>23</sup>J. N. Sweet, E. P. Roth, and M. Moss, *International Journal of Thermophysics* **8**, 593 (1987).
- <sup>24</sup>C. Hart, C. Skinner, A. Capece, and B. Koel, *Journal of Nuclear Materials* **468**, 71 (2016).
- <sup>25</sup>F. P. Incropera and D. P. DeWitt, *Fundamentals of Heat and Mass Transfer* (Wiley, New York, 1985).
- <sup>26</sup>V. J. Slabinski and R. L. Smith, *Review of Scientific Instruments* **42**, 1334 (1971).
- <sup>27</sup>C. R. Vidal and J. Cooper, *Journal of Applied Physics* **40**, 3370 (1969).